Energy and Buildings, *15 - 16* (1990/91) 861 - 874

A Numerical Analysis of Moisture Behavior in a Porous Wall by Quasilinearized Equations

MAMORU MATSUMOTO and YOSHITAKA TANAKA

Department of Environmental Planning, Faculty of Engineering, Kobe University, Rokko, Nada, Kobe 657 (Japan)

ABSTRACT

In order to predict the performance and to estimate the durability of building materials, an understanding of the behavior of heat and moisture in them, especially the maximum value of the moisture state of each material, is required. The governing equations are the system of heat- and moisture-transfer equations. These equations are nonlinear, because their coefficients are strongly dependent on dependent variables such as moisture content. If the system can be approximated by quasilinearized equations with adequate accuracy, a solution can be obtained simply by applying the superposition principle.

In this paper, quasilinearized time-variant equations are derived, and the allowable range of approximation of the linearized equations is discussed. The system of quasilinearized equations is obtained by expanding the original nonlinear equations around the reference solutions. After the nonlinear equations have been solved under reference boundary conditions, the quasilinearized equations are solved under the variation of the boundary value. The sum of the two solutions (the reference solution and the solution of the linearized equation) is the approximate solution. To determine the allowable range of approximation, two cases of variation of the boundary value, which are a step function and a sinusoidal function with a period of one year, are calculated. The structure of the building wall treated here is an internally insulated autoclaved lightweight concrete (ALC) wall, and the outdoor climate is that of Osaka, Japan.

In the case of step function variation, the allowable range of application is ± 1 *°C and* $\pm 10^4$ *J/kg (the chemical potential of water). In the case of sinusoidal function variations, the linear approximate solutions show fair agreement with exact solutions within 1 K of amplitude and* 10^4 *J/kg. It has been shown that quasilinearization produces acceptable approximate solutions and is effective in the prediction of moisture variation in a building structure.*

INTRODUCTION

Generally, the governing equations which describe the heat- and moisture-transfer process in porous building elements are nonlinear except for special cases, such as the vapor flow control process which occurs under rather low moisture contents, and the saturated liquid water flow process. The transfer coefficient (moisture and heat conductivity) and moisture capacity are strongly dependent on state variables such as the moisture content [1–3]. Also these equations are to be solved under varying boundary values, such as outdoor weather conditions, indoor air temperature and humidity.

To solve the equations, tedious numerical calculations such as the finite-difference method are used. Furthermore, tedious computational efforts are needed to obtain the periodic steady-state solutions [4, 5] that are useful for the thermal and moisture design of the building envelope.

In order to avoid the difficulties and complexities of the nonlinearity of the governing equations, an approximation of these equations by means of a linear expansion for variations around their reference solutions is studied. The approximate equations are linear, but they are time variant.

In this paper, the approximate linear equations are represented, and the use of these equations is discussed. The accuracy of the approximation is discussed by means of a comparison between the exact and approximate solutions.

0378-7788/91/$3.50

For an internally insulated lightweight concrete wall, annual variations of temperature and moisture are calculated for different variations of the boundary values, such as a step function and a sinusoidal function. The approximate solutions of the linearized equations are compared with the exact solutions, and the degree of approximation is discussed.

THE GOVERNING EQUATIONS

The governing equations for describing heat and moisture transfer in porous building elements are as follows [6]. In these equations the chemical potential of water relative to free liquid water is used as the moisture transfer potential.

From the moisture mass balance

$$k(\mu, T)\frac{\partial \mu}{\partial t} = \nabla\lambda'_{\mu}(\mu, T)\cdot\nabla\mu + \nabla\lambda'_{T}(\mu, T)\cdot\nabla T \tag{1}$$

From heat balance

$$C(\mu, T)\frac{\partial T}{\partial t} = \nabla\lambda_{\mu}(\mu, T)\cdot\nabla\mu + \nabla\lambda_{e}(\mu, T)\cdot\nabla T \tag{2}$$

$$k(\mu, T) \doteqdot k(\mu) = \rho_W \cdot \frac{\partial \phi}{\partial \mu} \qquad C(\mu, T) \doteqdot C(\mu)$$

The gravitational force term is neglected in eqn. (1) because it is negligibly small compared to the chemical potential gradient of water. The boundary conditions at the surface of the building wall surrounded by ambient air are

$$-\lambda'_{\mu}(\mu, T)\cdot\frac{\partial \mu}{\partial n} - \lambda'_{T}(\mu, T)\cdot\frac{\partial T}{\partial n} = \alpha'_{\mu}(\mu, T)\cdot(\mu_0 - \mu) + \alpha'_{T}(\mu, T)\cdot(T_0 - T) \tag{3}$$

from the moisture mass balance and

$$-\lambda_{\mu}(\mu, T)\cdot\frac{\partial \mu}{\partial n} - \lambda_{e}(\mu, T)\cdot\frac{\partial T}{\partial n} = \alpha_{\mu}(\mu, T)\cdot(\mu_0 - \mu) + \alpha_{e}(\mu, T)\cdot(T_0 - T) + S \tag{4}$$

from heat balance.

At the interface of the layers of the building wall element, the boundary conditions are

$$\mu_1 = \mu_2 \tag{5}$$

$$T_1 = T_2 \tag{6}$$

$${}_1\lambda'_{\mu}(\mu, T)\cdot\frac{\partial \mu_1}{\partial n} + {}_1\lambda'_{T}(\mu, T)\cdot\frac{\partial T_1}{\partial n} = {}_2\lambda'_{\mu}(\mu, T)\cdot\frac{\partial \mu_2}{\partial n} + {}_2\lambda'_{T}(\mu, T)\cdot\frac{\partial T_2}{\partial n} \tag{7}$$

$${}_1\lambda_{\mu}(\mu, T)\cdot\frac{\partial \mu_1}{\partial n} + {}_1\lambda_{e}(\mu_1 T)\cdot\frac{\partial T_1}{\partial n} = {}_2\lambda_{\mu}(\mu, T)\cdot\frac{\partial \mu_2}{\partial n} + {}_2\lambda_{e}(\mu, T)\cdot\frac{\partial T_2}{\partial n} \tag{8}$$

The initial conditions are

$$\mu = f_{\mu}(x), \quad T = f(x) \text{ at } t = 0 \tag{9}$$

Physical parameters such as λ'_{μ} and λ'_{T} are strongly dependent on the chemical potential of water and the temperature. These parameters are particularly dependent on the former. The nonlinearity of the governing equations is due to the dependency of these coefficients on the state variables.

QUASILINEARIZATION OF THE EQUATIONS

Let $\tilde{\mu}$ and $\tilde{T}$ be the solutions of eqns (1)–(9). Other solutions under the different boundary values (${}_b\mu + \Delta\mu$, ${}_bT + \Delta T$) are written as μ and T. The differences between them, i.e., $\mu - \tilde{\mu}$ and $T - \tilde{T}$, are written as h_{μ} and h_T:

$$h_{\mu} = \mu - \tilde{\mu} \tag{10}$$

$$h_T = T - \tilde{T} \tag{11}$$

By expanding the second solutions μ, T around the first solutions $\tilde{\mu}, \tilde{T}$ by using the Taylor expansion (see ref. 7), linearized equations for the variations h_{μ}, h_T are obtained as follows, neglecting terms higher than the second order of h_{μ}, h_T (see refs. 8 and 9):

$$\begin{aligned} k(\tilde{\mu})\cdot\frac{\partial h_{\mu}}{\partial t} &= \nabla(\lambda'_{\mu}(\tilde{\mu}, \tilde{T})\cdot\nabla h_{\mu}) \\ &\quad + \nabla(\lambda'_{T}(\tilde{\mu}, \tilde{T})\cdot\nabla h_T) \\ &\quad + \left[\left(\frac{\partial \lambda'_{\mu}}{\partial \mu}\middle|\nabla\tilde{\mu} + \frac{\partial \lambda'_{T}}{\partial \mu}\middle|\nabla\tilde{T}\right)\cdot h_{\mu}\right] \\ &\quad + \left[\left(\frac{\partial \lambda'_{\mu}}{\partial T}\middle|\nabla\tilde{\mu} + \frac{\partial \lambda'_{T}}{\partial T}\middle|\nabla\tilde{T}\right)\cdot h_T\right] \\ &\quad - \frac{\partial k}{\partial \mu}\middle|\frac{\partial \tilde{\mu}}{\partial t}h_{\mu} + \left[\nabla(\lambda'_{\mu}(\tilde{\mu}, \tilde{T})\cdot\nabla\tilde{\mu})\right. \\ &\quad \left. + \nabla(\lambda'_{T}(\tilde{\mu}, \tilde{T})\cdot\nabla\tilde{T}) - k(\tilde{\mu})\cdot\frac{\partial \tilde{\mu}}{\partial t}\right] \end{aligned} \tag{12}$$

$$C(\tilde{\mu})\cdot\frac{\partial h_T}{\partial t}=\nabla(\lambda_\mu(\tilde{\mu},\tilde{T})\cdot\nabla h_\mu)+\nabla(\lambda_e(\tilde{\mu},\tilde{T})\cdot\nabla h_T)$$
$$+\left[\left(\frac{\partial\lambda_\mu}{\partial\mu}\middle|\nabla\tilde{\mu}+\frac{\partial\lambda_e}{\partial\mu}\middle|\nabla\tilde{T}\right)\cdot h_\mu\right]$$
$$+\left[\left(\frac{\partial\lambda_\mu}{\partial T}\middle|\nabla\tilde{\mu}+\frac{\partial\lambda_e}{\partial T}\middle|\nabla\tilde{T}\right)\cdot h_T\right]$$
$$-\frac{\partial C}{\partial\mu}\middle|\frac{\partial\tilde{T}}{\partial t}h_\mu+\left[\nabla(\lambda_\mu(\tilde{\mu},\tilde{T})\cdot\nabla\tilde{\mu})\right.$$
$$\left.+\nabla(\lambda_e(\tilde{\mu},\tilde{T})\cdot\nabla\tilde{T})-C(\tilde{\mu})\cdot\frac{\partial\tilde{T}}{\partial t}\right] \tag{13}$$

The last terms on the right-hand sides of eqns. (12) and (13) are equal to zero, because each term is equal to eqn. (1) and eqn. (2), respectively. If eqns. (1) and (2) have been solved for $\tilde{\mu}$ and $\tilde{T}$, then the coefficients of eqns. (12) and (13) are known. These coefficients are functions of the time and space coordinates and are not dependent on the dependent variables h_μ, h_T. Equations (12) and (13) are linear and time-variant equations for the variables h_μ, h_T.

QUASILINEARIZED BOUNDARY CONDITIONS AND METHOD OF ANALYSIS

Suppose that the variations of the boundary values as outdoor or indoor air temperature and humidity are

$$\Delta\mu_b={}_b\mu_o-{}_b\tilde{\mu}_o \quad\text{or}\quad {}_b\mu_i-{}_b\tilde{\mu}_i \tag{14}$$

$$\Delta T_b={}_bT_o-{}_b\tilde{T}_o \quad\text{or}\quad {}_b\tilde{T}_i-{}_b\tilde{T}_i \tag{15}$$

where subscripts b, o and i mean boundary values, outdoor air and indoor air respectively. Let solutions of the nonlinear eqns. (1)–(9) under the boundary values ${}_b\mu$, ${}_bT$ be μ, T. In the following those solutions are termed exact solutions. Quasilinearized boundary conditions are obtained by expanding around the reference solutions $\tilde{\mu}$, $\tilde{T}$, which are the solutions under the boundary values ${}_b\tilde{\mu}$, ${}_b\tilde{T}$:

$$-\lambda'_\mu(\tilde{\mu},\tilde{T})\cdot\frac{\partial h_\mu}{\partial n}-\lambda'_T(\tilde{\mu},\tilde{T})\cdot\frac{\partial h_T}{\partial n}$$
$$=\alpha'_\mu(\tilde{\mu},\tilde{T})\cdot(\Delta\mu_b-h_\mu)$$
$$+\alpha'_T(\tilde{\mu},\tilde{T})\cdot(\Delta T_b-h_T)$$
$$+\left[\frac{\partial\alpha'_\mu}{\partial\mu}\middle|({}_b\tilde{\mu}-\tilde{\mu})+\frac{\partial\alpha'_T}{\partial\mu}\middle|({}_b\tilde{T}-\tilde{T})\right.$$
$$\left.+\frac{\partial\lambda'_\mu}{\partial\mu}\middle|\frac{\partial\tilde{\mu}}{\partial n}+\frac{\partial\lambda'_T}{\partial\mu}\middle|\frac{\partial\tilde{T}}{\partial n}\right]\cdot h_\mu$$
$$+\left[\frac{\partial\alpha'_\mu}{\partial T}\middle|({}_b\tilde{\mu}-\tilde{\mu})+\frac{\partial\alpha'_T}{\partial T}\middle|({}_b\tilde{T}-\tilde{T})\right.$$
$$\left.+\frac{\partial\lambda'_\mu}{\partial T}\middle|\frac{\partial\tilde{\mu}}{\partial n}+\frac{\partial\lambda'_T}{\partial T}\middle|\frac{\partial\tilde{T}}{\partial n}\right]\cdot h_T$$
$$+\left[\alpha'_\mu(\tilde{\mu},\tilde{T})\cdot({}_b\tilde{\mu}-\tilde{\mu})\right.$$
$$+\alpha'_T(\tilde{\mu},\tilde{T})\cdot({}_b\tilde{T}-\tilde{T})$$
$$\left.+\lambda'_\mu(\tilde{\mu},\tilde{T})\cdot\frac{\partial\tilde{\mu}}{\partial n}+\lambda'_T(\tilde{\mu},\tilde{T})\cdot\frac{\partial\tilde{T}}{\partial n}\right] \tag{16}$$

$$-\lambda_\mu(\tilde{\mu},\tilde{T})\cdot\frac{\partial h_\mu}{\partial n}-\lambda_e(\tilde{\mu},\tilde{T})\cdot\frac{\partial h_T}{\partial n}$$
$$=\alpha_\mu(\tilde{\mu},\tilde{T})\cdot(\Delta\mu_b-h_\mu)$$
$$+\alpha_e(\tilde{\mu},\tilde{T})\cdot(\Delta T_b-h_T)$$
$$+\left[\frac{\partial\alpha_\mu}{\partial\mu}\middle|({}_b\mu-\tilde{\mu})+\frac{\partial\alpha_e}{\partial\mu}\middle|({}_b\tilde{T}-\tilde{T})\right.$$
$$\left.+\frac{\partial\lambda_\mu}{\partial\mu}\middle|\frac{\partial\tilde{\mu}}{\partial n}+\frac{\partial\lambda_e}{\partial\mu}\middle|\frac{\partial\tilde{T}}{\partial n}\right]\cdot h_\mu$$
$$+\left[\frac{\partial\alpha_\mu}{\partial T}\middle|({}_b\tilde{\mu}-\tilde{\mu})+\frac{\partial\alpha_e}{T}\middle|({}_b\tilde{T}-\tilde{T})\right.$$
$$\left.+\frac{\partial\lambda_\mu}{\partial T}\middle|\frac{\partial\tilde{\mu}}{\partial n}+\frac{\partial\lambda_e}{\partial T}\middle|\frac{\partial\tilde{T}}{\partial n}\right]\cdot h_T$$
$$+[\alpha_\mu(\tilde{\mu},\tilde{T})\cdot({}_b\tilde{\mu}-\tilde{\mu})$$
$$+\alpha_e(\tilde{\mu},\tilde{T})\cdot({}_b\tilde{T}-\tilde{T})+S$$
$$\left.+\lambda_\mu(\tilde{\mu},\tilde{T})\cdot\frac{\partial\tilde{\mu}}{\partial n}+\lambda_e(\tilde{\mu},\tilde{T})\cdot\frac{\partial\tilde{T}}{\partial n}\right] \tag{17}$$

The last terms on the right-hand sides of eqns. (16) and (17) are equal to the reference boundary conditions (eqns. (3) and (4) respectively) and thus are equal to zero.

The initial conditions without variations of the initial values are

$$h_\mu=0 \quad\text{and}\quad h_T=0 \quad\text{at } t=0 \tag{9'}$$

Solving the quasilinearized eqns. (12) and (13) for dependent variables h_μ, h_T with the quasilinearized boundary conditions of eqns. (16) and (17) and the initial condition of eqn. (9'), the solutions h_μ, h_T are obtained. These equations are linear but time variant, which means that impulse response is a function of absolute time t. Since these eqns. (12)–(17) are linear, the superposition theorem can be applied.

Approximate solutions are obtained through the summation of the solutions of the

linearized equation (h_μ,h_T) under a variation of the boundary value ($\Delta\mu, \Delta T$) and the solution of the nonlinear equation ($\tilde{\mu}$, $\tilde{T}$) under the reference boundary value ($_b\tilde{\mu}$, $_b\tilde{T}$):

$$\mu \doteqdot \tilde{\mu} + h_\mu \tag{18}$$

$$T \doteqdot \tilde{T} + h_T \tag{19}$$

NUMERICAL ANALYSIS AND RESULTS

In this section, the moisture and temperature behaviors of the building wall under variations of the boundary values are calculated by using the linearized equations. The results are compared with exact solutions calculated with the original nonlinear equations. The degree of approximation under different variations of the boundary values is discussed.

(1) Numerical analysis method

The calculations are performed by using a finite-difference method of implicit Crank–Nicholson type. Linearized eqns. (12)–(17) and (9′) are solved simultaneously with the original eqns. (1)–(4) and (9). In each time step, the difference equations of the original nonlinear equations for ($\tilde{\mu}$, $\tilde{T}$) are solved under the reference boundary value, then the difference equations of the linearized equations for variations h_μ, h_T are solved using the reference solutions $\tilde{\mu}$, $\tilde{T}$ obtained above [10, 11].

(2) Structure of the building wall and properties of materials

The structure of the building element calculated is the internally insulated lightweight concrete wall shown in Fig. 1.

For ease of calculation in this analysis, the thin water barrier on the outer surface of the wall, the insulation layer and the fiberboard layer on the inside are treated as layers having no moisture and heat capacity when the annual cycle of the boundary value

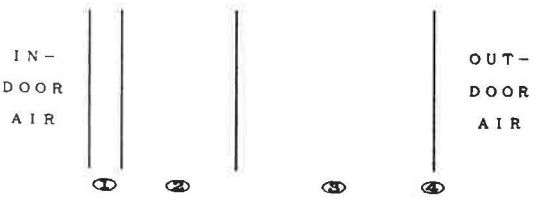

Fig. 1. The structure of the wall. ① Fiberboard, 5 mm; ② insulation, 5 cm; ③ ALC, 10 cm; ④ water barrier.

TABLE 1

Heat and moisture resistances of materials, air layers and the sum of all resistances

Materials and air layers	Heat resistance (m^2 K/W)	Moisture resistance (m^2 s Pa/kg)
Indoor:		
Indoor air layer	0.108	8.00E + 9
Fiberboard	1.22	4.82E + 8
Insulation	0.0538	3.42E + 8
Total	1.38	8.82E + 9
Outdoor:		
Outdoor air layer	0.0431	8.58E + 8
Water barrier		8.00E + 9
Total	0.0431	8.86E + 9

is taken into account. Then, they can be treated as pure resistance layers for moisture and heat flow ($\tilde{\alpha}'^{-1}$, $\tilde{\alpha}^{-1}$). Since moisture flow through these layers is vapor controlled, each value of the moisture resistance related to the vapor pressure difference is a constant value independent of the moisture content and temperature. The values used in the calculations are shown in Table 1.

The physical parameters of the lightweight concrete are shown in Figs. 2–4. Figure 2 shows the equilibrium relation between the chemical potential of water and the moisture content at 290 K. Based on the theory of liquid flow in a bundle of capillaries, the liquid moisture conductivity related to the temperature gradient

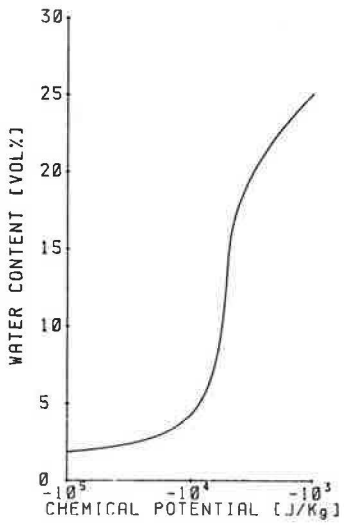

Fig. 2. Equilibrium relation between chemical potential of water and water content at 20 °C.

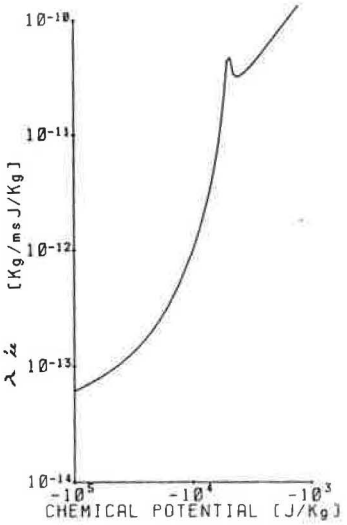

Fig. 3. Dependence of the coefficient of moisture conductivity λ'_{μ} on water content at 20 °C.

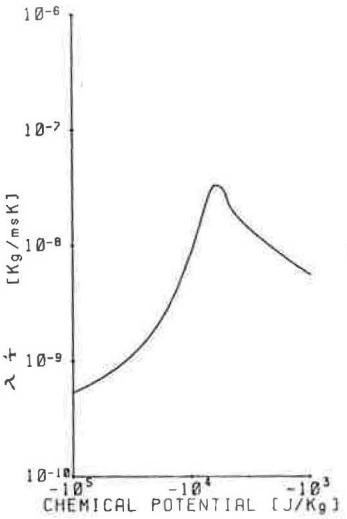

Fig. 4. Dependence of the coefficient of moisture conductivity λ'_T on water content at 20 °C.

$\lambda'_{T\mathrm{l}}$ is assumed to be zero. Then $\lambda'_{T\mathrm{g}} = \lambda'_T$. Using Stefan's law for vapor flow, $\lambda'_{\mu\mathrm{g}}$ is related to λ'_{T_g} as follows:

$$\lambda'_{\mu\mathrm{g}} = \lambda'_{T\mathrm{g}} \cdot \frac{(\partial P_\mathrm{V}/\partial\mu)_T}{(\partial P_\mathrm{V}/\partial T)_\mu}$$

$$= \lambda'_{T\mathrm{g}}/[(\partial P_{\mathrm{VS}}/\partial T) \cdot (R_\mathrm{V} \cdot T/P_{\mathrm{VS}}) - \mu/T]$$

Using the relation and values of $\lambda'_{T\mathrm{g}}$ shown in Fig. 4, values of $\lambda'_{\mu\mathrm{g}}$ are obtained (Fig. 3). The values of the moisture conductivity mentioned above are dependent on the temperature. The dependence of these coefficients ($\lambda'_{\mu\mathrm{g}}$, $\lambda'_{T\mathrm{g}}$, $\lambda'_{\mu\mathrm{l}}$) on temperature is estimated by applying the classical models of Stefan's law for vapor phase flow and Darcy's law for liquid phase flow, respectively. $\lambda'_{\mu\mathrm{g}}$ is linearly dependent on the saturated vapor pressure P_{VS}, and $\lambda'_{T\mathrm{g}}$ is dependent on P_{VS} and its derivative $\partial P_{\mathrm{VS}}/\partial T$. $\lambda'_{\mu\mathrm{l}}$ depends slightly on temperature and is directly proportional to ρ_W/η, where η is the viscosity of liquid water. Values of those conductivities for each temperature are calculated by using the relationship mentioned above.

(3) Boundary values for the reference solution

Reference boundary values are as follows:

outdoor air:

$$_\mathrm{b}\tilde{T}_\mathrm{o} = {}_\mathrm{b}T_{\mathrm{o,a}} + 11.3\sin(\omega t) \tag{20}$$

$$_\mathrm{b}\tilde{\mu}_\mathrm{o} = R_\mathrm{V} \cdot {}_\mathrm{b}T_\mathrm{o} \cdot \ln[{}_\mathrm{b}RH_{\mathrm{o,a}} + A\sin(\omega t)] \tag{21}$$

where subscript a means average value and ${}_\mathrm{b}T_{\mathrm{o,a}} = 288.76$ K, ${}_\mathrm{b}RH_{\mathrm{o,a}} = 0.66$, $\omega = 2\pi/365 \times 24 \times 3600\ \mathrm{s}^{-1}$. Time $t = 0$ is at 8 a.m., May 1. The coefficient A is:

(i) $A = 0.11$: 8 a.m., May 1 $\leqslant t <$ 8 a.m., October 1.

(ii) $A = 0$: 8 a.m., October 1 $\leqslant$ 8 a.m., May 1.

indoor air:

$$_\mathrm{b}\tilde{T}_\mathrm{i} = 293.16 \tag{22}$$

$$_\mathrm{b}\tilde{\mu}_\mathrm{i} = R_\mathrm{V} \cdot {}_\mathrm{b}T_\mathrm{i} \cdot \ln(0.7) \tag{23}$$

The boundary values of outdoor air vary with the annual period. In this calculation, the daily variation is discarded for simplicity.

(4) Variations of the boundary value

The step function and sinusoidal function of the annual cycle are used for the variation of the boundary value ($\Delta\mu$, ΔT). Taking into account the linearity of the linearized equation, solutions of the linearized equation are calculated under a unit magnitude function (Heaviside unit function and sinusoidal function with unit amplitude) as the variation of the boundary value, of which solutions are the unit response or the unit frequency response (see refs. 12 and 13). The solution for an arbitrary value of the magnitude is obtained by multiplying the magnitude by the unit response or the unit frequency response. Types of combinations of the boundary values in the calculations (cases 1–6) are shown in Table 2.

TABLE 2

Combinations of variations of boundary values

Variational function of boundary value	Case No.	Outdoor chemical potential	Outdoor air temperature	Indoor chemical potential	Indoor air temperature
Step function		10^4	0	0	0
		-10^4	0	0	0
		0	1	0	0
		0	-1	0	0
		0	0	10^4	0
	1	0	0	-10^4	0
		0	0	0	1
	2	0	0	0	-1
Sinusoidal function	3	$10^4 \sin \omega t$	0	0	0
	4	0	$\sin \omega t$	0	0
	5	0	0	$10^4 \sin \omega t$	0
	6	0	0	0	$\sin \omega t$

(5) Results of calculations

The limit of the application of the approximate solution mentioned above is discussed, comparing the approximate solution $(h_\mu + \tilde{\mu}, h_T + \tilde{T})$ with the exact solution (μ, T). The comparison of the solutions is performed under various magnitudes of the variation of the boundary value.

(a) The case of a step function

Comparison of the approximate solution with the exact solution is performed during the second year, when the effects of the initial conditions have almost disappeared (almost periodic steady state). The results of calculations of case 1 and case 2 are shown in Figs. 5–9 and Figs. 10–14, respectively.

In the structure treated here, the moisture flow through the outer surface of the ALC is about 10^{-1} to 10^{-2} times the moisture flow through the inner surface of the ALC. The change of moisture potential in ALC depends mainly on the moisture potential of room air. As shown in Fig. 5, the front of the moisture potential wave travels from the inside of the ALC to the outside. The maximum moisture

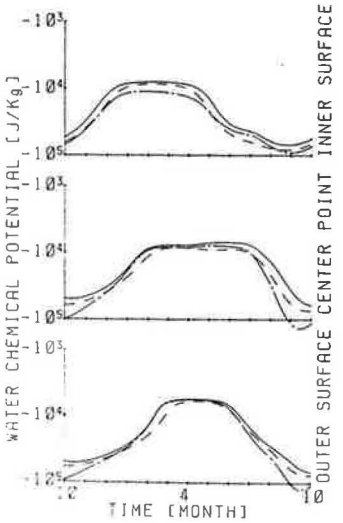

Fig. 5. The change of chemical potential of water during the second year (case 1). ——, reference solution; – – –, exact solution; – · – · –, approximate solution.

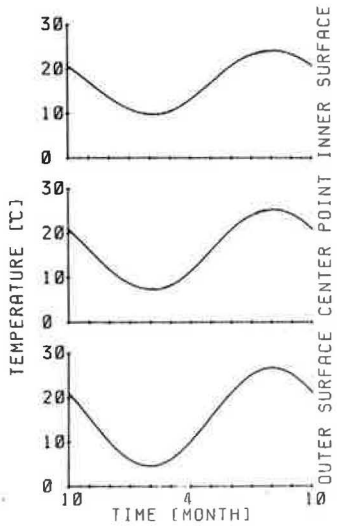

Fig. 6. The change of temperature during the second year (case 1). ——, reference solution; – – –, exact solution; – · – · –, approximate solution.

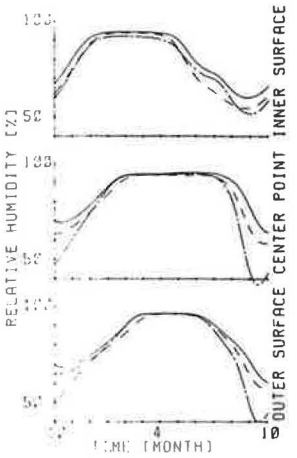

Fig. 7. The change of relative humidity during the second year (case 1). ——, reference solution; – – –, exact solution; – · – · –, approximate solution.

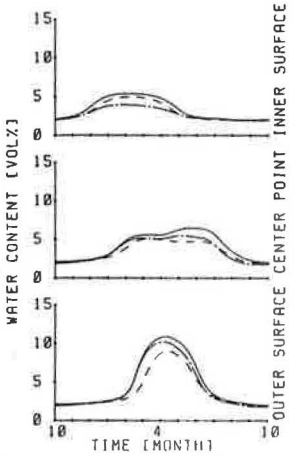

Fig. 8. The change of water content during the second year (case 1). ——, reference solution; – – –, exact solution; – · – · –, approximate solution.

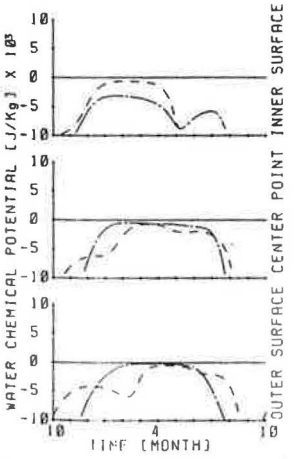

Fig. 9. The change of the deviation of the water chemical potential during the second year (case 1). ——, reference solution; – – –, exact solution; – · – · –, approximate solution.

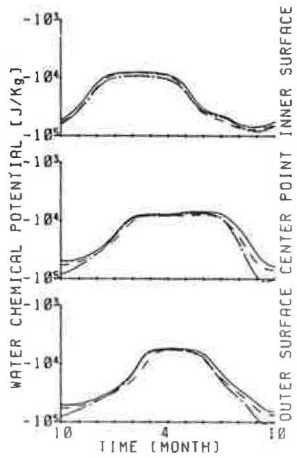

Fig. 10. The change of chemical potential of water during the second year (case 2). ——, reference solution; – – –, exact solution; – · – · –, approximate solution.

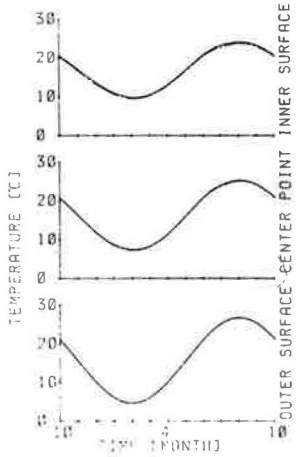

Fig. 11. The change of temperature during the second year (case 2). ——, reference solution; – – –, exact solution; – · – · –, approximate solution.

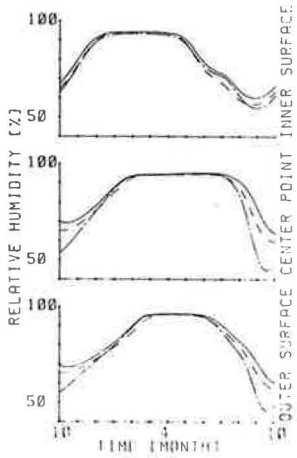

Fig. 12. The change of relative humidity during the second year (case 2). ——, reference solution; – – –, exact solution; – · – · –, approximate solution.

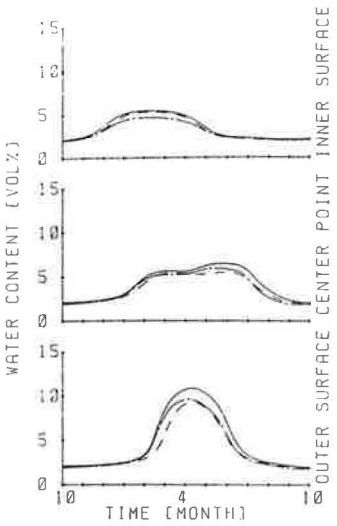

Fig. 13. The change of water content during the second year (case 2). ——, reference solution; – – –, exact solution; – · – · –, approximate solution.

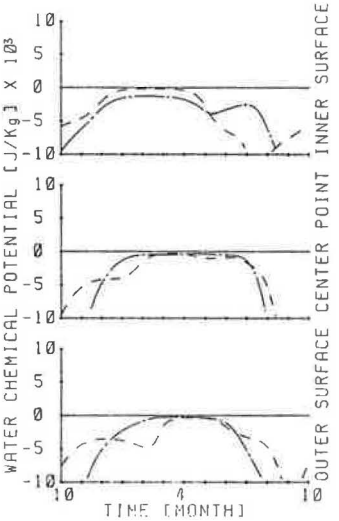

Fig. 14. The change of the deviation of water chemical potential during the second year (case 2). ——, reference solution; – – –, exact solution; – · – · –, approximate solution.

potential in the ALC layer occurs at the outer surface of the ALC in April. The duration of the high moisture potential is longest at the middle part of the wall. The moisture potential in the ALC layer decreases with a decrease in the indoor air moisture potential. A comparison of the exact solution with the reference solution shows that the amount of decrease of the moisture potential during the wetting period (during the period of higher moisture potential) is least at the outer surface of the ALC, where the maximum moisture potential in ALC exists. The decrease of moisture potential during the drying period is larger than that during the wetting period.

In case 1, the approximate solution shows good agreement with exact solution, as shown in Figs. 5 and 9. The difference between the exact and approximate solutions of the chemical potential in winter tends to be larger during the drying period. The result for the relative humidity is shown in Fig. 7. Figure 8 shows the change of moisture content calculated using the value of the chemical potential of water and the temperature. The difference between the approximate and exact solutions is small during the dry period. For temperature, the approximate solution coincides with the exact solution (Fig. 6). The results of case 2 (Figs. 10–14) are similar to those of case 1. During the wetting period, the approximate solutions show good agreement with the exact solution, especially at the outer surface of the ALC where the maximum moisture potential exists. The criteria for evaluating the hydric design of the wall are the maximum moisture potential and the duration. From these results, it can be concluded that the approximate solution is sufficiently accurate within $\pm 10^4$ J/kg of water chemical potential variation and ± 1 K of temperature variation, and the limit of application of the approximate solution is $\pm 10^4$ J/kg and ± 1 K. Because of the linearity of the linearized equations, solutions h_μ under $\Delta T_i = 1, \Delta T_o = 0$ are equal to solutions under $\Delta T_i = 0, \Delta T_o = -1$, and so on.

The same results were obtained for other cases in Table 2, but will not be presented here.

(b) The case of a sinusoidal function

The results of cases 3, 4, 5 and 6 are shown in Figs. 15–19, Figs. 20–24, Figs. 25–29 and Figs. 30–34, respectively.

The approximate solutions show good agreement with the exact solutions. The difference between the approximate solution and the exact solution for the chemical potential of water is relatively large in the period from June to November in comparison with other periods (Figs. 15, 20, 25 and 30). As shown in Figs. 24, 29 and 34, h_μ based on the linearized equation shows a larger deviation during the rapidly increasing or decreasing period of the chemical potential of water. The same feature appeared in the relative

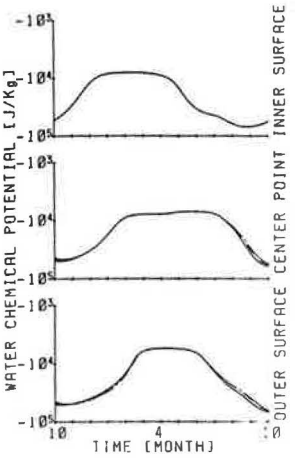

Fig. 15. The change of chemical potential of water during the second year (case 3). ——, reference solution; – – –, exact solution; – · – · –, approximate solution.

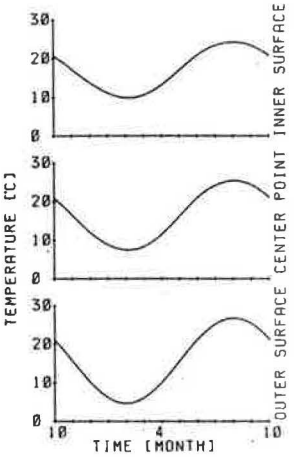

Fig. 16. The change of temperature during the second year (case 3). ——, reference solution; – – –, exact solution; – · – · –, approximate solution.

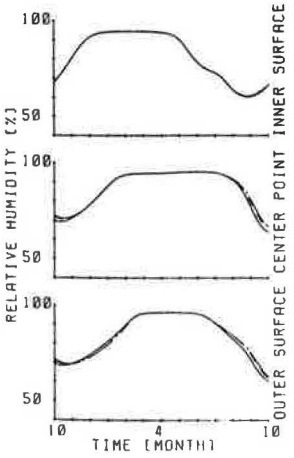

Fig. 17. The change of relative humidity during the second year (case 3). ——, reference solution; – – –, exact solution; – · – · –, approximate solution.

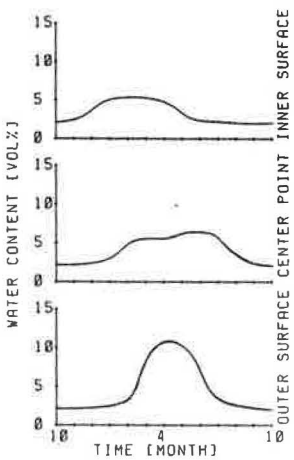

Fig. 18. The change of water content during the second year (case 3). ——, reference solution; – – –, exact solution; – · – · –, approximate solution.

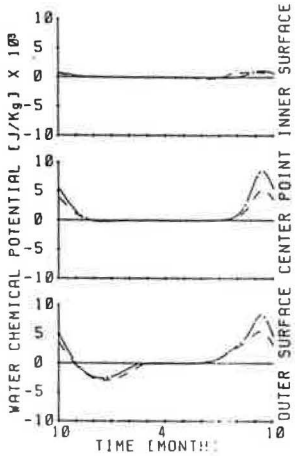

Fig. 19. The change of the deviation of water chemical potential during the second year (case 3). ——, reference solution; – – –, exact solution; – · – · –, approximate solution.

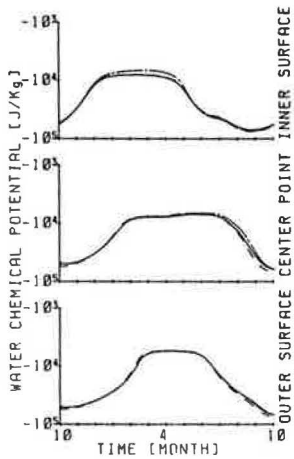

Fig. 20. The change of chemical potential of water during the second year (case 4). ——, reference solution; – – –, exact solution; – · – · –, approximate solution.

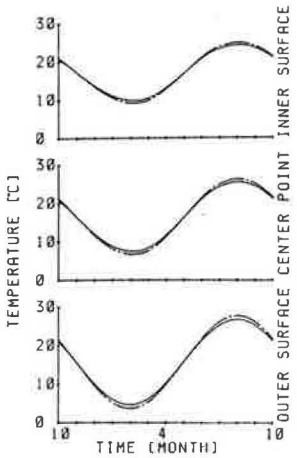

Fig. 21. The change of temperature during the second year (case 4). ——, reference solution; – – –, exact solution; – · – · –, approximate solution.

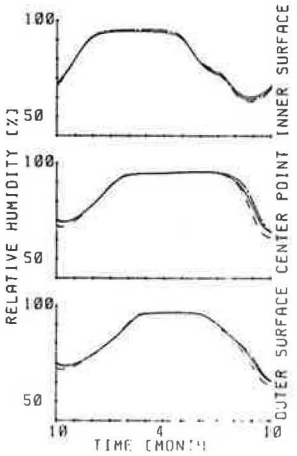

Fig. 22. The change of relative humidity during the second year (case 4). ——, reference solution; – – –, exact solution; – · – · –, approximate solution.

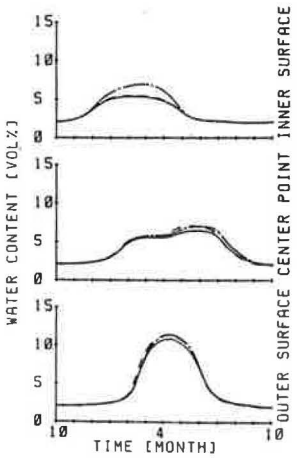

Fig. 23. The change of water content during the second year (case 4). ——, reference solution; – – –, exact solution; – · – · –, approximate solution.

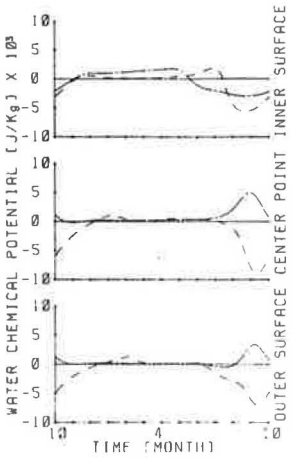

Fig. 24. The change of deviation of water chemical potential during the second year (case 4). ——, reference solution; – – –, exact solution; – · – · –, approximate solution.

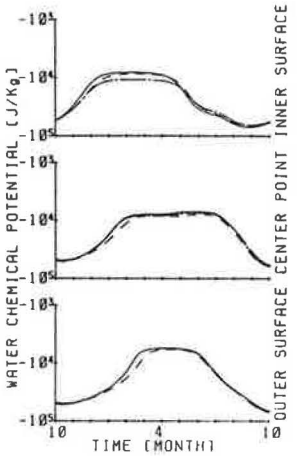

Fig. 25. The change of chemical potential of water during the second year (case 5). ——, reference solution; – – –, exact solution; – · – · –, approximate solution.

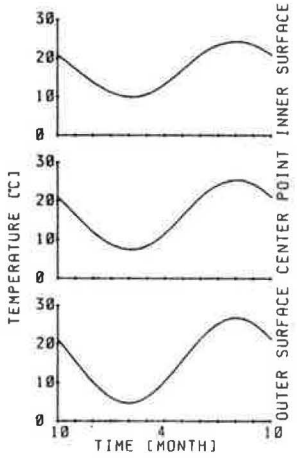

Fig. 26. The change of temperature during the second year (case 5). ——, reference solution; – – –, exact solution; – · – · –, approximate solution.

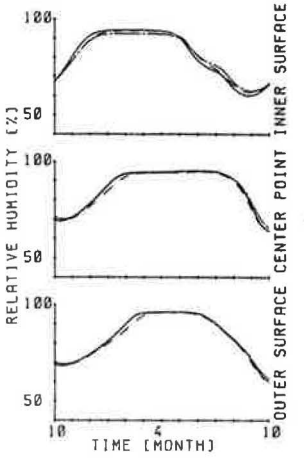

Fig. 27. The change of relative humidity during the second year (case 5). ——, reference solution; – – –, exact solution; – · – · –, approximate solution.

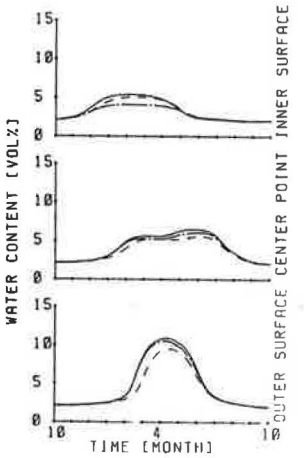

Fig. 28. The change of water content during the second year (case 5). ——, reference solution; – – –, exact solution; – · – · –, approximate solution.

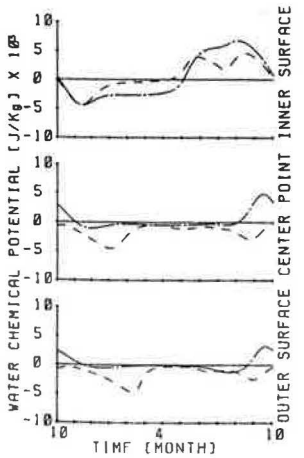

Fig. 29. The change of the deviation of water chemical potential during the second year (case 5). ——, reference solution; – – –, exact solution; – · – · –, approximate solution.

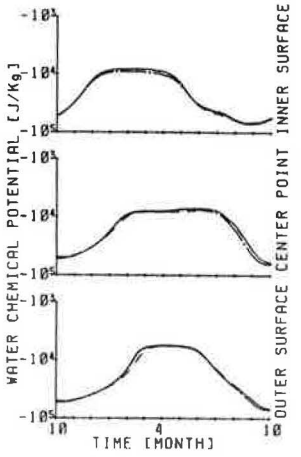

Fig. 30. The change of chemical potential of water during the second year (case 6). ——, reference solution; – – –, exact solution; – · – · –, approximate solution.

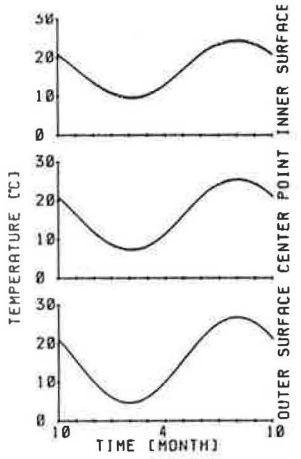

Fig. 31. The change of temperature during the second year (case 6). ——, reference solution; – – –, exact solution; – · – · –, approximate solution.

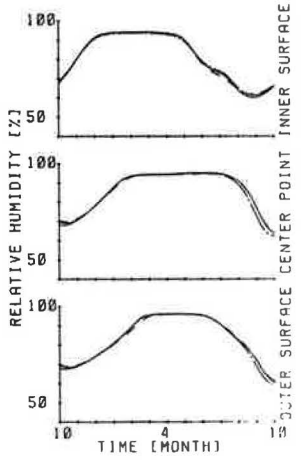

Fig. 32. The change of relative humidity during the second year (case 6). ——, reference solution; – – –, exact solution; – · – · –, approximate solution.

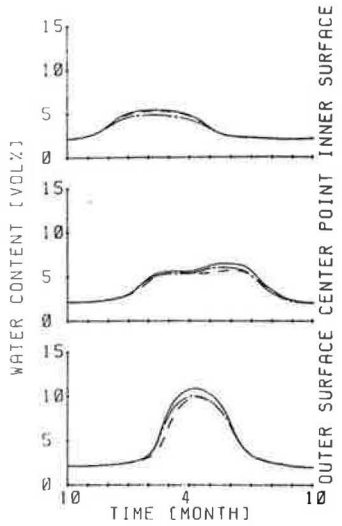

Fig. 33. The change of water content during the second year (case 6). ——, reference solution; – – –, exact solution; – · – · –, approximate solution.

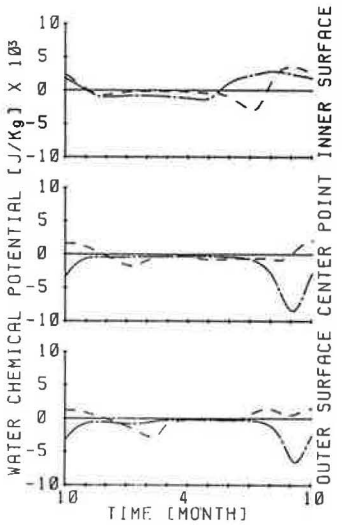

Fig. 34. The change of the deviation of water chemical potential during the second year (case 6). ——, reference solution; – – –, exact solution; – · – · –, approximate solution.

humidity (Figs. 17, 22, 27 and 32). The approximate solutions for the temperature coincide with the exact solutions (Figs. 16, 21, 26 and 31). Figures 18, 23, 28 and 33 show the change of water content during the second year. These results reveal that the limit of application is 10^4 J/kg of amplitude in the chemical potential of water and 1 K of amplitude in temperature.

CONCLUSIONS

(1) Quasilinearized equations around the reference solutions of the original nonlinear equations are derived for solving the heat- and moisture-flow problem in building physics and for evaluating the thermal and hydric design of a building wall. The approximate solution is given by the sum of the solution of the nonlinear equation under a reference boundary value and the solution of the linearized equation on variation of the boundary value.

(2) Comparing the approximate solution with the exact solution, the allowable range of application of the linearized equations is discussed for an internally insulated lightweight concrete wall. A step function and an annually cyclic sinusoidal function are used for variations of the boundary values. In the case of a step function the allowable range of approximation is $\pm 10^4$ J/kg in variation of water chemical potential and ± 1 K in temperature variation. In the case of a sinusoidal function, the allowable range of approximation is 10^4 J/kg of amplitude in the chemical potential of water and 1 K of amplitude in temperature. 10^4 J/kg in water chemical potential is equivalent to about 5% in relative humidity at 290 K. From these results, moisture prediction by the linearized equation is useful in the hydric and thermal design of a building wall.

(3) The limit of the approximation depends on the structure of the building wall and the physical parameters.

NOMENCLATURE

$C = c\rho$	heat capacity of wet material (J/m³ K)
c	specific heat of wet material (J/kg)
h_T	variation of temperature (K)
h_μ	variation of chemical potential of water (J/kg)
P_V	partial water vapor pressure (Pa)
P_{VS}	saturated water vapor pressure (Pa)
RH	relative humidity
R_V	universal gas constant of water (J/kg K)

r the sensible heat of water vaporization (J/kg)
S surface heat production (W/m^2)
T temperature (K)
t time (s)
x, n space coordinate (m)

Greek Symbols

α total thermal transfer coefficient (W/m^2 K)
$\tilde{\alpha}^{-1}$ total thermal transfer resistance (inner air layer + inner surface cover + insulation layer + outer air layer) (m^2 K/W)
α' moisture transfer coefficient related to partial vapor pressure (kg/m^2 s Pa)
$\tilde{\alpha}'^{-1}$ total moisture transfer resistance related to partial vapor pressure (inner air layer + inner surface cover + insulation layer + moisture proof layer + outer air layer) (m^2 s Pa/kg)
$\alpha_e = \alpha + r\alpha'_T$ effective thermal transfer coefficient (W/m^2 K)
$\alpha'_T = \alpha' P_V / T$ moisture transfer coefficient related to temperature (kg/m^2 s K)
$\alpha_\mu = r\alpha'_\mu$ thermal transfer coefficient related to water chemical potential (W/(m^2 J/kg))
$\alpha'_\mu = \alpha' P_V / T$ moisture transfer coefficient related to water chemical potential (kg/(m^2 s J/kg))
η kinetic viscosity of liquid water (m^2/s)
λ thermal conductivity coefficient (W/m K)
$\lambda_e = \lambda + r\lambda'_{Tg}$ effective thermal conductivity (W/m K)
$\lambda'_T = \lambda'_{Tg} + \lambda'_{Tl}$ total moisture conductivity coefficient for temperature gradient (kg/m s K)
λ'_{Tg} moisture conductivity coefficient in gas phase for temperature gradient (kg/m s K)
λ'_{Tl} moisture conductivity coefficient in liquid for temperature gradient (kg/m s K)
$\lambda'_\mu = \lambda'_{\mu g} + \lambda'_{\mu l}$ total moisture conductivity coefficient for water chemical potential gradient (kg/(m s J/kg))
$\lambda'_{\mu g}$ moisture conductivity coefficient in gas phase for water chemical potential gradient (kg/(m s J/kg))
$\lambda'_{\mu l}$ moisture conductivity coefficient in liquid phase for water chemical potential gradient (kg/(m s J/kg))
$\mu = R_V T \times \ln(P_V/P_{VS})$ water chemical potential (Gibbs' free energy) (J/kg)
ρ density (kg/m^3)
ρ_W density of liquid water (kg/m^3)
ϕ water content (vol.%)
$\omega = 2\pi/(365 \times 24 \times 3600)$ frequency of boundary values (s^{-1})
$\Delta\mu = {}_b\mu - {}_b\tilde{\mu}$
$\Delta T = {}_bT - {}_b\tilde{T}$

Subscripts and Superscripts

a average
b boundary value
i indoor
o outdoor
W water
1, 2 material number
reference value

REFERENCES

1 J. R. Philip and D. A. deVries, Moisture movement in porous materials under temperature gradient, *Trans. Am. Geophys. Union*, *38* (1957) 222–232.
2. W. Jury, Simultaneous transport of heat and moisture through a medium sand, *Ph.D. Thesis*, Wisconsin University, 1973.
3. M. Matsumoto, Simultaneous heat and moisture transfer equations for porous building materials under moisture condensation and analysis of the process, *Proc. Heat Transfer Symp. Architectural Inst. Jpn., Environmental Eng.*, *6* (1976) 15–27 (in Japanese).
4. M. Matsumoto and M. Sato, Numerical analysis of moisture content in the multi-layered building wall during the internal moisture condensation and reevaporation, *Trans. Environmental Eng. in Architecture, Architectural Inst. Jpn.*, *4* (1982) 153–158 (in Japanese).
5. M. Matsumoto and M. Sato, The periodic solution of

moisture condensation and reevaporation process in building wall, *4th Int. Conf. Numerical Method in Thermal Problems, 1985, Numerical Method in Thermal Problems*, 1985, Vol. 2, pp. 819–829.
6. M. Matsumoto, *Moisture, Building Physics*, Vol. 10, *Physics of Environment*, Shoukokusha, Tokyo 1984 (in Japanese).
7. T. Y. Na, An initial value method for the solution of class of nonlinear equations in fluid mechanics, *J. Basic Eng. Trans. ASME*, (1970) 503–509.
8. M. Matsumoto, Method of analysis of moisture condensation and evaporation in building wall, *Proc. Heat Transfer Symp. Architectural Inst. Jpn., Environmental Eng., 12* (1982) 41–50 (in Japanese).
9. M. Matsumoto, Quasilinearization of nonlinear heat and moisture transfer equations and parameter sensitivity analysis, *Proc. Architectural Inst. Jpn., Kinki (Planning Environmental Eng.), 26* (1986) 109–112 (in Japanese).
10. M. Matsumoto and H. Nagai, Analysis of moisture variation in building wall by quasilinearization, *Proc. Architectural Inst. Jpn., Kinki (Planning and Environmental Eng.), 27* (1987) 9–12 (in Japanese).
11. M. Matsumoto and H. Nagai, An analysis of moisture variation in building wall by quasilinearized equations of nonlinear heat and moisture equations, *CIB W-40 Meeting, Boräs, 1987.*
12. M. Matsumoto and Y. Tanaka, Analysis of heat and moisture movement of internally insulated building wall by quasilinearized equations, *Proc. Architectural Inst. Jpn., Kinki (Planning and Environmental Eng.), 28* (1988) 209–212 (in Japanese).
13. M. Matsumoto and Y. Tanaka, Analysis of heat and moisture movement of internally insulated building wall by quasilinearized equations for various variations of boundary conditions, *Proc. Architectural Inst. Jpn., Kinki (Planning and Environmental Eng.), 29* (1989) 77–80 (in Japanese).